ISSN 1330-3651(Print), ISSN 1848-6339 (Online)
https://doi.org/10.17559/TV-00000000000000
Categorization of paper (Style: Ariel Narrow, 8pt)

Influence of Clay Block Masonry Properties on the Out-of-Plane Behaviour of Infilled RC Frames

Filip ANIĆ, Davorin PENAVA, Damir VAREVAC, Vasilis SARHOSIS

Abstract: In order to determine the characteristics that govern the out-of-plane behaviour of masonry infills, two groups of wall specimens were build and tested in the laboratory. Specimens were assembled and tested as described in EN 1052-2 provisions and constitute of flexural strength for a plane of failure parallel and perpendicular to the bedjoints specimens. By obtaining data from experiments, numerical micromodels developed to predict their mechanical behaviour. A calibration procedure undertaken and results obtained from the experimental campaign found to be in agreement with those obtained from the numerical models. Additionally, former in-plane infilled frame numerical models were tested with acquired out-of-plane calibrated material model. No significant difference was found.

Keywords: clay block masonry infill, out-of-plane behaviour, flexural test, micromodels

1 INTRODUCTION

Reinforced concrete (RC) frames infilled with unreinforced masonry units (URM) is a common structural practice in seismically active South Europe (Booth & Key, 2006). European earthquake design provisions Eurocode 8 (CEN, 2004b) regard wall infill/panels as an secondary elements, i.e. they do not contribute to overall seismic behaviour. However, it was known that infills contribute in seismic behaviour of RC frames even in the late 1960's. From there, interest in seismic behaviour of infilled frames has grown (Asteris et al., 2017; Trapani et al., 2015; Asteris et al. 2016) on separate fields of in-plane (IP) loading, out-of-plane (OOP) loading and their combination (IP + OOP). A large amount of experimental and analytical studies have been done in the field of IP, the same cannot be stated for the OOP and especially for IP + OOP interaction (Asteris et al., 2017; Wang et al. 2016). Moreover, the OOP field is based on analytical research of arching action, and numerical, i.e. computational research is scares and is based on membrane and strut with centred mass models.

Consequently, this paper is a part of OOP research with the intention to account properties that determine behaviour of infills subjected to OOP loading. Accordingly, 20 masonry wall specimens were tested and numerical micro models calibrated to account the experiment.

2 METHODS, MATERIALS AND RESULTS OF TESTED WALL SPECIMENTS

2.1. Experiment preparation

The experiment preparation and testing was done in accordance to EN 1052-2 (British Standards Institution, 2016). Two testing groups were made: Group I: flexural strength for a plane of failure parallel to the bedjoints, and Group II: flexural strength for a plane of failure perpendicular to the bedjoints (parallel to headjoints). The recommendation of 10 wall test specimens for each Group was adopted in favour of statistical significance (Sorić, 2016). Wall specimens are made from whole and half-length blocks (fig.2).

Firstly, hollow clay masonry units (fig.1a) were cut in half of their height (fig.1b) to emulate the units used as an infill in RC frames testing from (Penava, 2012) and units that will be used in further experiments.

Mortar joints have designated M5 class according to EN 1996-1-1 (CEN, 2005) and nominal 10 mm thickness.

Pretested properties of clay blocks, mortar and wall specimens are presented on the table 1.

Test setup of masonry wall specimens can be seen on a figure 2, 4c & 4f. The average dimensions of 10 specimens in each group as well as test setup dimensions are shown on figure 2. Testing was conducted with an increasing monotonic load on a 4-point (2 line reactions + 2 line loads) load setup on Controls 50-C1201/BFR by 50-C1200/8 apparatus.

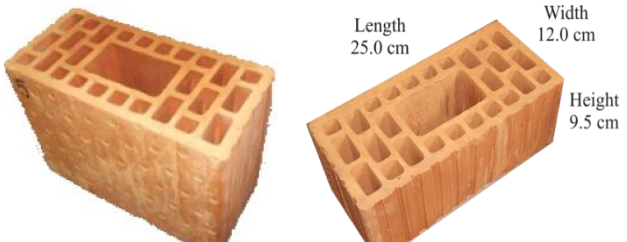

a) Original clay block b) Modified clay block

Figure 1 Masonry unit

Table 1 Pretested mechanical properties (Penava, 2012)

Entity	Properties	Value	Unit
Clay block	f_b	15.90	MPa
	f_{bh}	2.60	MPa
Mortar	f_m	5.15	MPa
	f_{mt}	1.27	MPa
Wall specimen	f_k	2.70	MPa
	E	3900.00	MPa
	ε_u	0.58	‰
	f_{vk0}	0.35	MPa
	$tg\alpha_k$	0.24	MPa

It was expected that Group I will fail by separating two rows of blocks on bedjoint at the mid-height of the specimen. Hence, reaching tensile strength of the mortar. On the other hand, two possible failures were expected for the Group II. Those include: a) separation of blocks by

mortar (blocks are undamaged) or b) failure trough the specimens (blocks failed). The b) failure is more likely to happen as $f_{mt} > f_{bh}$.

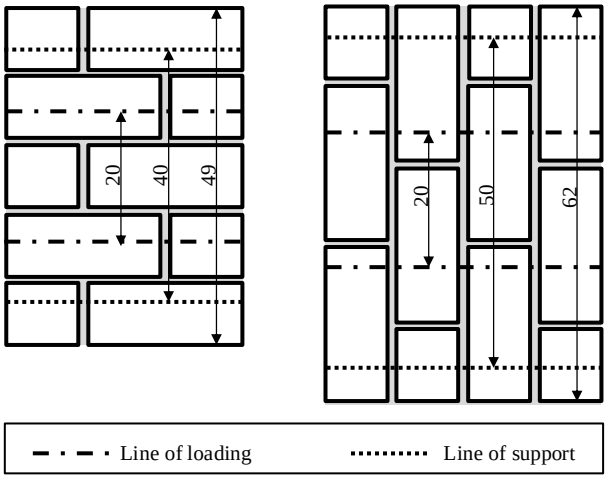

a) Group I b) Group II

Figure 2 Test setup mesurement

2.2. **Experimental results**

Averaged results of the conducted test can be seen on table 2 & its distribution on figure 3. Figure 3 shows the minimum (MIN), maximum (MAX) and mean strength (AVG) with its variation within standard deviation (straight lines), i.e. $f_x \pm s$. Flexural strength was calculated by equation 1 from (British Standards Institution, 2016). Group I failed by separation of block rows by the bedjoint at the specimens mid-height (fig4d&e). Group II failed by failing clay blocks (fig4g&h), hence, through the whole wall specimen.

Table 2 Mean reults from flexular test

Properties	Group I	Group II	Unit
F_{max}	4.07	6.69	kN
f_x (eq.1)	0.21	0.38	MPa
s	0.07	0.06	MPa
c_v	0.28	0.18	/

$$f_x = \frac{3F_{max}(l_1 - l_2)}{2bt} \quad (1)$$

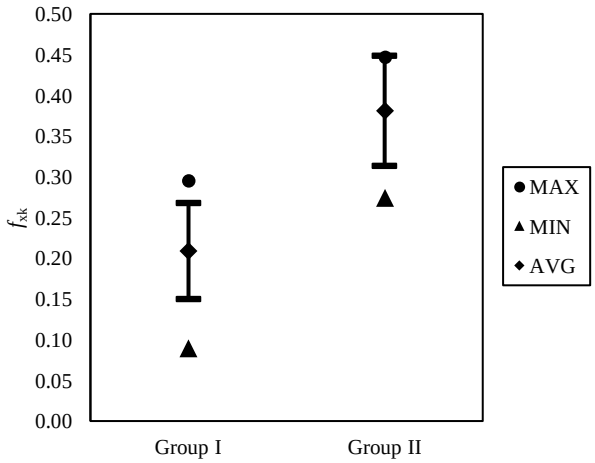

Figure 3 Strenght distribution

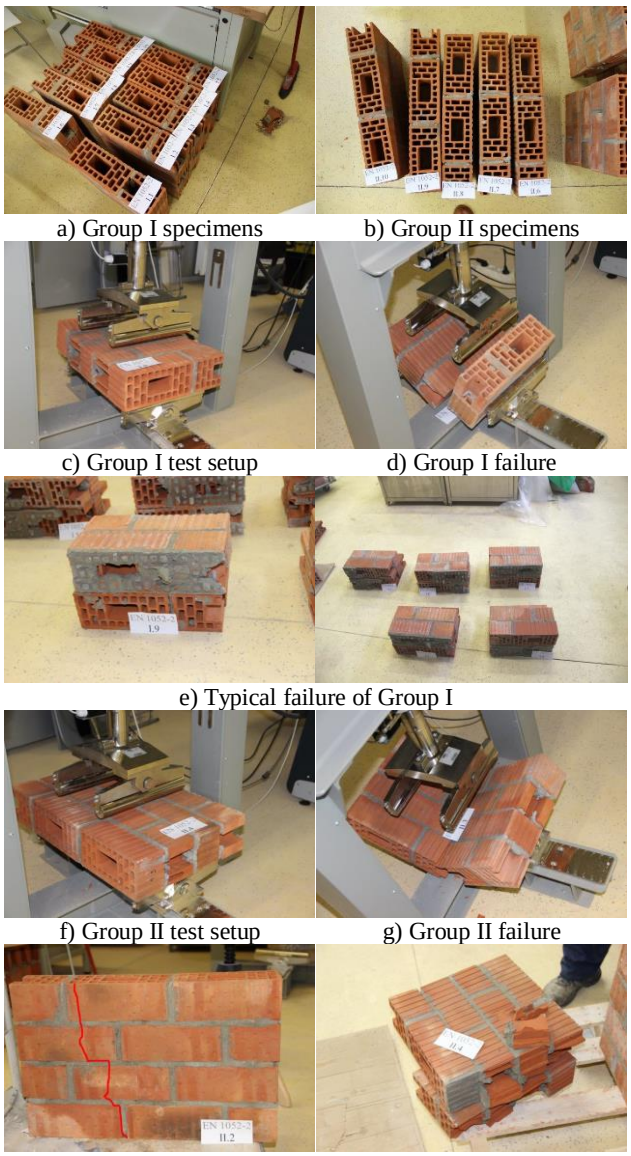

Figure 4 Test setup and failure modes

3. METHODS, MATERIALS AND RESULTS OF NUMERICAL MODEL

3.1. Numerical model

Numerical models were assembled and tested using Atena 3D Eng (Cervenka Consulting, 2015). A three-dimensional micromodeling approach was used, constructed from three-dimensional solid and two-dimensional contact – interface (zero thickness) elements (fig.5). The construction of numerical model was carried out by assembling solid elements that have dimensions same as the real clay masonry unit (fig.1), they are jointed by zero thickness interface elements, thus, the dimensions of the numerical model and real specimens (fig.2) differ. Distance between loading (fig.6) was adopted as in experiments.

Figure 6 shows numerical model with its boundary conditions. The wall specimens were simply supported and loaded with uniform continuous line load in –z direction. When uniform loads form figure 6 are

multiplied by their length of their span, the force corresponds to 0.5 kN/step force each.

Furthermore, solid elements beyond the supports in the numerical model (fig.6) were discarded in order to gain faster calculation time. It is to be noted that the calculation with solids continuing beyond the supports was carried out, and no significant differences was observed from those without solids beyond supports.

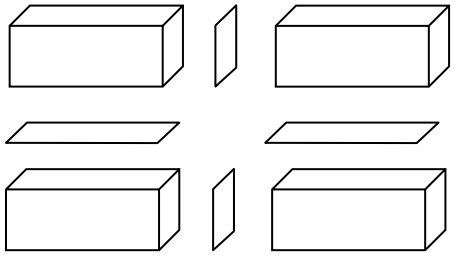

3D Solid + 2D Interface + 3D Solid

Figure 5 Micromodel composition

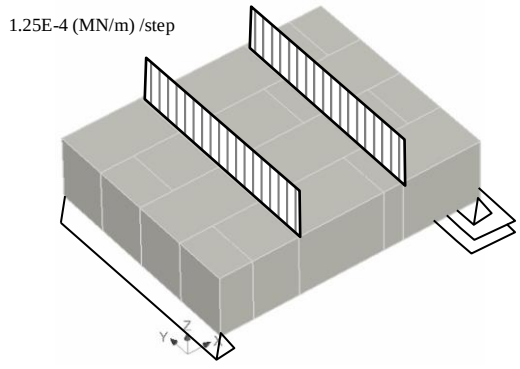

a) Group I

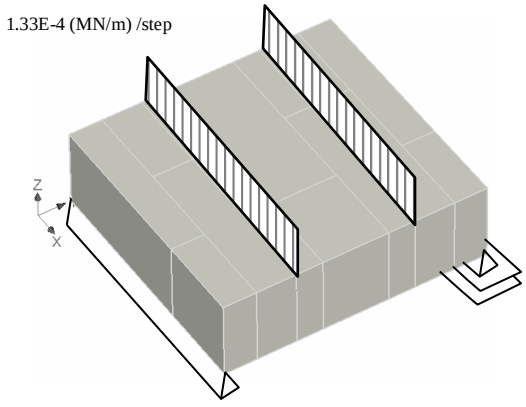

b) Group II

Figure 6 Numerical model setup

3.2. Numerical material models and calibration

Numerical material models (tab.3&4) were adopted form (Penava, Sigmund, & Kožar, 2016) and modified during the calibration. The CC nonlinear cementitious 2 material model from table 3 was used for modelling clay masonry units, hence, solid elements. Likewise, CC interface material model from table 4 was used to model the mortar joints, hence, 2D interface gap elements. The interlocking effect of mortar filling the voids of opposite blocks and thereby locking them is modelled by interlocking function (fig.7).

Table 3 CC Nonlinear Cementitious 2 model **(Cervenka, Jendele, & Cervenka, 2012)**

Properties	Value	Unit
E	5.650E+03	MPa
μ	0.100	/
f_t	0.380	MPa
f_c	-1.750E+01	MPa
G_f (eq.1)	4.500E-04	MN/m
W_d	-5.000E-04	/
ε_{cp}	-1.358E-03	/
$r_{c,lim}$	0.800	/
S_F	20.000	/
Crack model coefficient	1.000	/

Table 4 CC 3D interface model (Cervenka et al., 2012)

Symbol	Mortar bedjoint	Mortar headjoint	Unit
	Value	Value	
K_{nn} (eq.2)	5.65E+05	8.50E+04	MN/m2
K_{tt} (eq.3)	2.57E+05	3.86E+04	MN/m2
f_t	0.20	0.20	MPa
c	0.35	0.35	MPa
tgα	0.24	0.24	/
Interlocking	see fig.7	/	

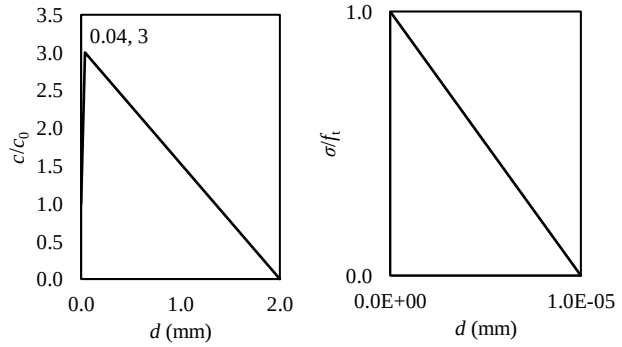

a) Interlock function b) Tension softening

Figure 7 Interface functions

$$G_f = 0.000025\, f_t \quad (1)$$

$$K_{nn} = E / t \quad (2)$$

$$K_{tt} = G / t \quad (3)$$

The mentioned models from (Penava et al., 2016) acquire properties of clay blocks in direction of voids, however, during the analysis of the results from conducted numerical tests they were inadequate for modelling of Group II, i.e. the response was higher than measured by experiments. To that end, changes to tensile

strength and tension softening function was introduced. Tensile strength was changed from that in the direction of voids f_t = 1.80 MPa to that of perpendicular to the voids f_t = 0.38 MPa as the OOP loading caused failure of the clay blocks in direction perpendicular to voids. The displacement tension softening function through trial and error was adjusted from d = 0.010 mm to d = 0.001 mm. Fracture energy calculation depends upon tensile strength (eq.1) (Vos, 1983), however it was left unchanged, i.e. as if tensile strength in eq.1 was is in the direction of voids. If tensile strength in eq.1 was changed to be perpendicular to the voids, a predeveloped failure occurs in both Groups.

3.3. Numerical test results

With changes to the material models, the results from numerical tests are shown on figure 8 and table 5. Table 5 shows the force at failure and maximal principal stress obtained from figure 8.

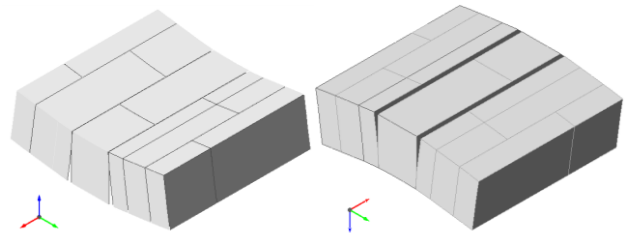

a) Deformed model Group I

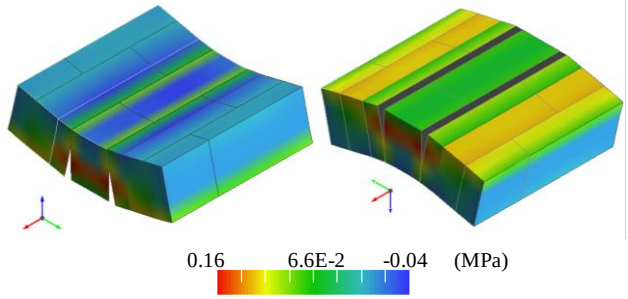

b) Max. principal stress Group I

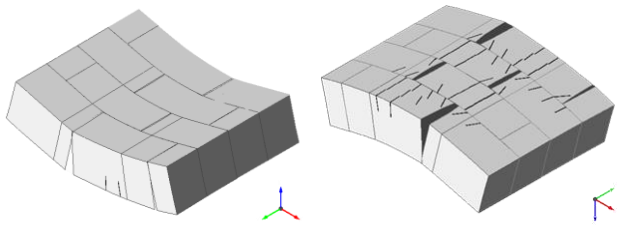

c) Deformed model Group II

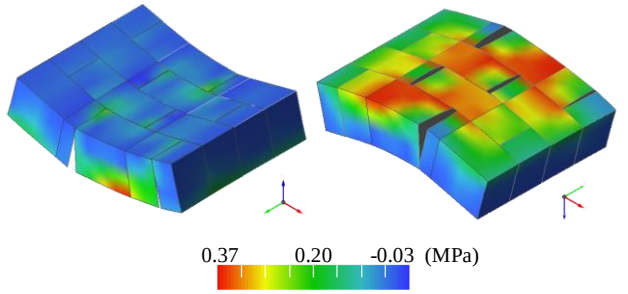

d) Max. principal stress Group II

Deformation × 300	Min. crack width 0.001 mm
Crack width multiplier ×1	Shift crack outwards ×0

Figure 8 Numerical test results at F_{max}

Table 5 Results from numerical tests

Group	F_{max} (kN)	σ_{max} (MPa)
I	4.50	/
II	6.20	0.37

By Figure 8a it can be observed that numerical model of Group I had failure by discontenting bedjoints, i.e. mortar tensile failure. Figure 8c shows failures and cracking of the clay blocks.

4. ADDITIONAL INVESTIGATION ON INFILED FRAME

4.1. General information

Having material model properties changed, previous work with unreinforced masonry infilled (URM) RC frames (Anić, Penava, Legatiuk, & Sarhosis, 2017; Anić, Penava, & Sarhosis, 2017; Sarhosis 2016) was questioned. Hence, the modifications to the infill units were implemented into the infilled frame model in order to measure the possible alterations. In short, the reinforced concrete (RC) frame has a designated medium ductility class (DCM) by Eurocode 2 provisions (CEN, 2004a), boundary conditions with numerical test setups are presented on figure 9. The model was subjected as in previous works (in-plane pushover method). For more details on the infilled frame please refer to the (Anić, Penava, & Sarhosis, 2017) article.

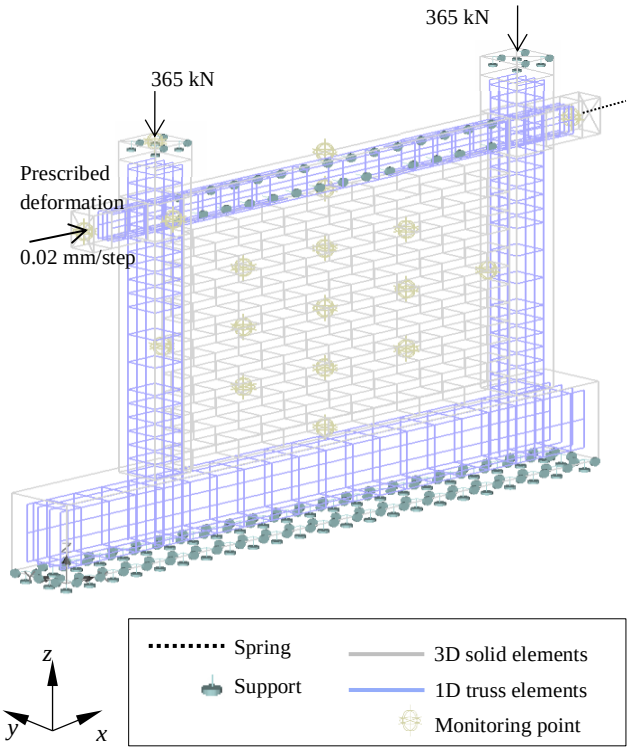

Figure 9 Infilled frame numerical model.

4.2. Infilled frame numerical test results

Force displacement diagrams of both infill material models are shown on figure 10. Cracks and minimal principal stresses for each of the two are shown on figure 11.

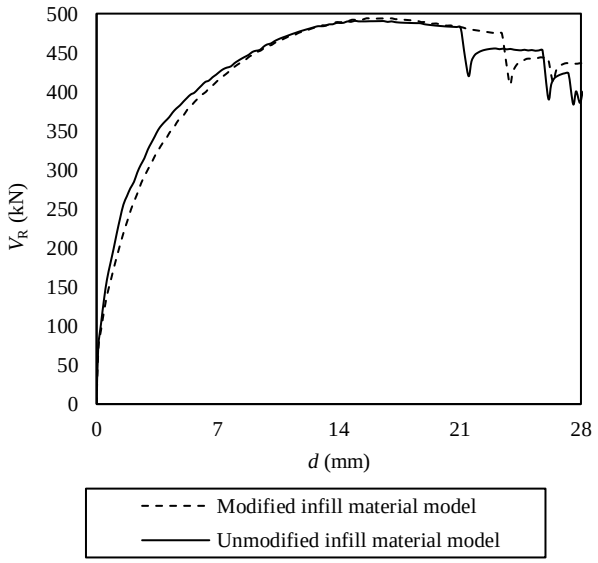

Figure 10 Force displacement diagram of infilled frame model

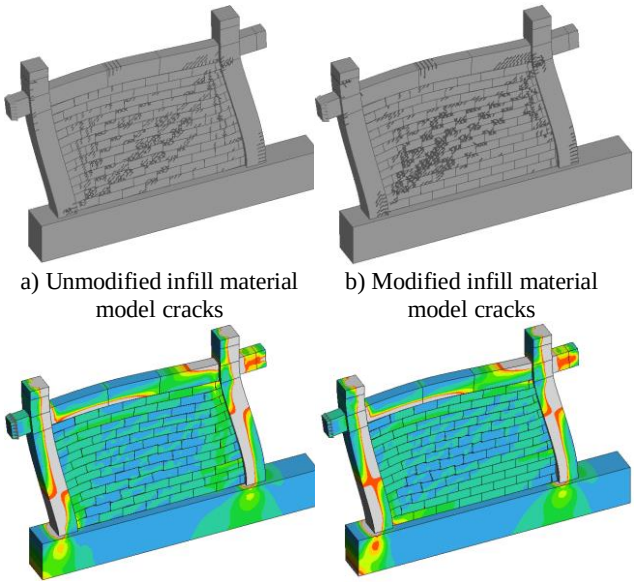

a) Unmodified infill material model cracks

b) Modified infill material model cracks

c) Unmodified infill material model min. principal stress

d) Modified infill material model min. principal stress

Deformation scale ×10		Crack width multiplier	×1
Min. crack width	1E-4 m	Shift cracks outwards	0

Figure 11 Infilled frame numerical model results at d = 28 mm

5. CONCLUSIONS AND DISCCUSION OF THE RESULTS

By comparing numerical and experimental results of Group I & II, differences force-wise were calculated as 9.55% for Group I and 7.32% for Group II. Group II has stress-wise difference of 2.63%.

Based on flexural testing of masonry wall specimens a numerical model was compiled and calibrated. Calibration included modifying tension strength and displacement in tension softening function. Tension strength was changed from the value in direction of voids to the value perpendicular to voids. The calibration has proven adequate enough to have high correlation with the experiments. It is to be noted that the calibration was carried out in favour of Group II as Group I due the specific failure mode (reaching tensile strength of mortar) had agreement with the experiments from beginning.

Additionally, an infilled framed was tested in order to observe the validity due to changes in material model of clay blocks. It was shown that the changes did not drastically affect the outcome force (fig.10), crack and stress wise (fig.11).

In summation, the following conclusions can be drawn:

a) Wall specimens had failure modes as predicted, Group I had failure along bedjoints due to reaching mortar tensile strength. Group II failed along the blocks, reaching tensile strength of the blocks in direction perpendicular to the voids.

b) In order to simulate OOP bending, a mix of mechanical properties had to be implemented into the material models. Tensile strength of clay masonry unit was set to have the value perpendicular to the voids, end displacement in tension softening function was lowered, other properties have mechanical values in direction of voids.

c) Numerical models of Group I & II had failure mechanism same as the experimental ones (fig.4&8). Likewise, the numerical results force and stress wise have satisfying degree of agreement.

d) When the load is parallel to bedjoints, governing element are the bedjoints, more exactly mortars tensile strength. On the other hand, when the load is parallel to headjoints, the governing elements are properties of the clay block, i.e. its tensile strength.

e) The changes of material models had no significant effect on the URM frame model in regards to crack and stress pattern as well as force – displacement curve.

f) Regarding the changes to numerical model of clay masonry block and its unneglectable effect to the IP pushover analysis of URM frames it obvious that the main governing element of URM frames are interfaces, more exactly bedjoint.

6. LIST OF SYMBOLS

Test specimens	
l_1	Distance between supports
l_2	Distance between loading
b	Specimens length
t	Specimens thickness
Mechanical (tested) properties	
f_b	Clay blocks normalized compression strength in direction of voids
f_{bh}	Clay blocks normalized compression strength in direction perpendicular to voids
f_m	Mortars compressive strength
f_{mt}	Mortars flexural strength

f_k	Characteristic masonry wall compressive strength
E	Elastic modulus of wall specimen
ε_u	Ultimate wall strain
f_{vk0}	Initial shear strength
$tg\alpha_k$	Friction coefficient
f_{x1}	Flexural strength for a plane of failure parallel to the bedjoints – Group I
f_{x2}	Flexural strength for a plane of failure perpendicular to the bedjoints (parallel to headjoints) – Group II
s	Standard deviation (STDEV)
c_v	Variation coefficient

Numerical material properties

E	Elastic Modulus
μ	Poisson's coefficient
f_t	Tensile strength
f_c	Compressive strength
G_f	Fracture Energy
W_d	Plastic displacement
ε_{cp}	Strain at f_c
$r_{c,lim}$	Maximal strength reduction under the large transverse strain
S_F	Shear factor coefficient that defines a relationship between normal and shear crack stiffness.
K_{nn}	Normal interface stiffness
K_{tt}	Tangential interface stiffness
c	Cohesion
$tg\alpha$	Friction coefficient
V_R	Shear force
d	Displacement

7. REFERENCES

Anić, F., Penava, D., Legatiuk, D., & Sarhosis, V. (2017). Influence of variability in materials used on seismic response of masonry infilled reinforced concrete frames. In *Osmi susret Hrvatskog društva za mehaniku* (pp. 1–9). Osijek, Croatia. Retrieved from http://bib.irb.hr/prikazi-rad?rad=885880

Anić, F., Penava, D., & Sarhosis, V. (2017). Development of a three-dimensional computational model for the in-plane and out-of-plane analysis of masonry-infilled reinforced concrete frames. In *6th International Conference on Computational Methods in Structural Dynamics and Earthquake Engineering*. Rhodes Island, Greece.

Asteris, P. G., Cavaleri, L., Di Trapani, F., & Tsaris, A. K. (2017). Numerical modelling of out-of-plane response of infilled frames: State of the art and future challenges for the equivalent strut macromodels. *Engineering Structures*, *132*, 110–122. https://doi.org/10.1016/j.engstruct.2016.10.012

Asteris PG, Cavaleri L, Di Trapani F, Sarhosis V. A macro-modelling approach for the analysis of infilled frame structures considering the effects of openings and vertical loads. Structure and Infrastructure Engineering 2016, 12(5), 551-566.

Booth, E. D., & Key, D. (2006). *Earthquake Design Practice for Buildings*. Cambridge: Thomas Telford. Retrieved from http://ebooks.cambridge.org/ref/id/CBO9781107415324A009

British Standards Institution. (2016). Methods of test for masonry Part 2: Determination of flexural strength. *Bs En 1052-2*.

CEN. (2004a). *Eurocode 2: Design of concrete structures - Part 1-1: General rules and rules for buildings (EN 1992-1-1:2004)*. Brussels: European Committee for Standardization.

CEN. (2004b). *Eurocode 8: Design of Structures for Earthquake Resistance - Part 1: General Rules, Seismic Actions and Rules for Buildings (EN 1998-1:2004)*. Brussels: European Committee for Standardization.

CEN. (2005). *Eurocode 6: Design of masonry structures - Part 1-1: General rules for reinforced and unreinforced masonry structures (EN 1996-1-1:2005).* Brussels: European Committee for Standardization.

Cervenka, V., Jendele, L., & Cervenka, J. (2012). *ATENA Program Documentation Part 1 Theory*. Prague: Cervenka Consulting Ltd.

Cervenka Consulting. (2015). ATENA for Non-Linear Finite Element Analysis of Reinforced Concrete Structures. Prague: Červenka Consulting s.r.o.

Penava, D. (2012). *Influence of openings on seismic response of masonry infilled reinforced concrete frames*.

Penava, D., Sigmund, V., & Kožar, I. (2016). Validation of a simplified micromodel for analysis of infilled RC frames exposed to cyclic lateral loads. *Bulletin of Earthquake Engineering*, *14*(10), 2779–2804. https://doi.org/10.1007/s10518-016-9929-0

Sarhosis V. An optimization procedure for material parameter identification in masonry constitutive models. International Journal of Masonry Research and Innovation 2016, 1(1), 48-58.

Sorić, Z. (2016). *Zidane konstrukcije*. Zagreb: Sveučilište u Zagrebu.

Trapani, F. Di, Macaluso, G., Cavaleri, L., Papia, M., Di, F., Macaluso, G., … Papia, M. (2015). Masonry infills and RC frames interaction : literature overview and state of the art of macromodeling approach. *European Journal of Environmental and Civil Engineering*, *19*(9). https://doi.org/10.1080/19648189.2014.996671

Vos, E. (1983). Influence of loading rate and radial pressure on bond in reinforced concrete. A numerical and experimental approach. *Thesis*.

Wang C, Forth JP, Nikitas N, Sarhosis V. Retrofitting of masonry walls by using a mortar joint technique; experiments and numerical validation. Engineering Structures 2016, 117, 58-70.

Contact information:

Filip ANIĆ, mag. ing. aedif
(Corresponding author)
Josip Juraj Strossmayer University of Osijek,
Faculty of Civil Engineering Osijek
Vladimira Preloga 3, 31000 Osijek, Croatia
filip.anic@gfos.hr

doc. dr. sc. Davorin PENAVA, dipl. ing. građ.
Josip Juraj Strossmayer University of Osijek,
Faculty of Civil Engineering Osijek
Vladimira Preloga 3, 31000 Osijek, Croatia
davorin.penava@gfos.hr

izv. prof. dr. sc. Damir VAREVAC, dipl. ing. građ.
Josip Juraj Strossmayer University of Osijek,
Faculty of Civil Engineering Osijek
Vladimira Preloga 3, 31000 Osijek, Croatia
damir.varevac@gfos.hr

doc. dr. sc. Vasilis SARHOSIS, dipl. ing. građ.
Newcastle University,
School of Engineering,
Drummond Building, Newcastle upon Tyne, NE1 7RU, United Kingdom
vasilis.sarhosis@ncl.ac.uk